Applied Catalysis A, General 650 (2023) 118997

Contents lists available at ScienceDirect

Applied Catalysis A, General

journal homepage: www.elsevier.com/locate/apcata

Evaluating the per site activity of common mesoporous materials as supports for aminosilica catalysts for the aldol reaction and condensation

Michael Brizes, Jee-Yee Chen, Hannah Pineault, Nicholas A. Brunelli *

The Ohio State University, William G. Lowrie Department of Chemical and Biomolecular Engineering, 151W. Woodruff Ave., Columbus, OH 43210, USA

ARTICLE INFO

Keywords:
SBA-15
MCM-41
Aldol reaction and condensation
Site quantification
Aminosilica
Mesoporous silica

ABSTRACT

Mesoporous silicas are regarded as ideal systems; however, they are complex. The materials can be functionalized with aminosilanes to produce highly active catalysts for aldol chemistry. Despite heterogeneous catalysts often having multiple sites, functionalized materials are tested assuming each site contributes equally to catalytic activity. Here, we functionalize common mesoporous silicas (MCM-41, MCM-48, and SBA-15) and determine the per site catalytic activity. The activity of functionalized MCM-41, MCM-48, and SBA-15 are similar if SBA-15 has negligible micropore volume (NMP-SBA-15). Site quantification data reveal that each material has four different types of sites. MCM-41 has the highest fraction of active sites; however, most sites are low activity. Interestingly, NMP-SBA-15 is as active as MCM-41. NMP SBA-15 has a higher fraction of high activity and medium activity sites than both MCM materials. Overall, each material has similar types of sites even though the materials have different pore structures and different pore sizes.

1. Introduction

The discovery of mesoporous silica materials has expanded the possibilities for high performance materials in many applications, including carbon capture, [1–5] drug delivery, [6,7] and heterogenous catalysis [8–12]. Mesoporous silica materials were developed with larger pores (i.e., pore sizes of 3–12 nm) to overcome diffusion limitations commonly encountered with microporous materials such as zeolites (pore sizes of <2 nm) with subsequent reports demonstrating that the materials are robust and tunable [13–15]. Two common mesoporous materials are SBA-15 [16,17] and MCM-41 [18,19] because they have simple structures and are readily synthesized. Both materials are promising supports for many applications in catalysis, including the aldol reaction and condensation (aldol chemistry) [9,20–23]. Yet, the mesoporous silica materials are complex [24]. Whereas recent work [20,21,23,25–32] has identified structure-function behavior that can improve the overall material design, the observations overlook the inherent complexity of these materials, considering the average catalytic activity rather than the per site catalytic activity. Considerable opportunity exists to create more active materials through investigating the catalytic activity of different mesoporous supports on a per site basis.

Aldol chemistry is an important reaction to form carbon-carbon bonds that can be used to produce valuable chemicals or upgrade biomass [33–37]. In nature, aldol chemistry is catalyzed by enzymes (*aldolases*) that selectively produce aldol adducts at ambient conditions [38,39]. The key to *aldolase* activity is that they catalyze aldol chemistry using cooperative interactions [40]. Cooperative interactions occur when two distinct moieties work in union to catalyze the reaction at a rate that is greater than the individual components [9,25,28,30,41]. Enzymes can achieve cooperative interactions through using simple functional groups such as a acids and bases. Translating these concepts to heterogeneous catalytic materials remains an important challenge.

As cooperative interactions can involve co-localized acid/base pairs, [21,25,28,30,42–44] a promising catalytic material includes an aminosilica material that contains a basic amine on a weakly acidic silanol covered silica surface. Similar to an enzyme, the co-location of the acid and base groups enable Aldol chemistry to be catalyzed by an enamine mechanism [45,46]. As depicted in Scheme 1, the current understanding is that there are beneficial cooperative interactions between an amine and a surface silanol at two points in the catalytic cycle: (1) when acid interacts with the oxygen of the ketone to facilitate nucleophilic attack by the amine and (2) when the acid interacts with the oxygen of the aldehyde to enable the enamine to attack the aldehyde to form the aldol adduct [29].

These cooperative interactions are affected by tuning the aminosilane structure [21,31,44] and reaction environment [20,27] since the

* Corresponding author.
E-mail address: brunelli.2@osu.edu (N.A. Brunelli).

https://doi.org/10.1016/j.apcata.2022.118997

Available online 11 December 2022

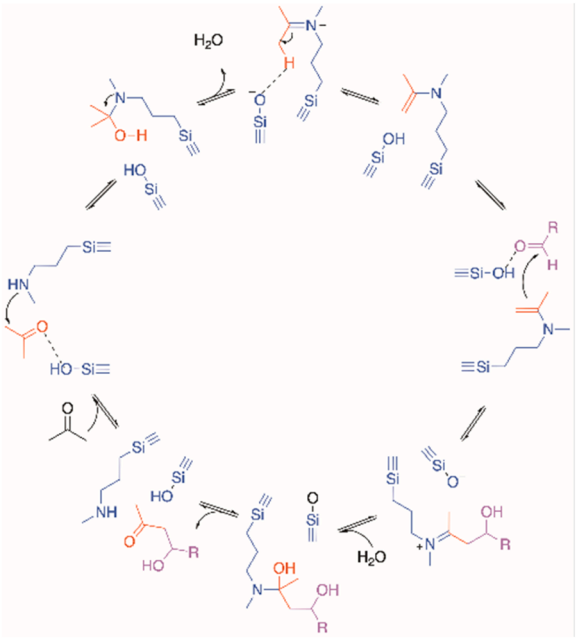

Scheme 1. Reaction mechanism for secondary amine catalyzed aldol chemistry involving the enamine intermediate.

reaction rate is influenced by the reaction medium, [26] type of amine, [26] substituent groups, [31] and alkyl linker length. [21,44] Whereas primary amines are more active in water, [26] secondary amines with a methyl group have been shown to be the most active aldol catalysts when the reaction occurs in an organic medium. [31] Moreover, changing the alkyl linker length of the aminosilane can influence the acid and base interactions by affecting the proximity of the amine and surface silanol. [21,44] It was found that using an alkyl linker length to a propyl (C3) linker enabled beneficial cooperative interactions for SBA-15 and MCM-41. [29] These structural factors of the aminosilane can influence the acid and base interactions that affect the observed catalytic activity for aldol chemistry.

Whereas many observations have been made for the aminosilane structure, the support structure has many tunable features that can influence the catalytic activity, including the presence of micropores and loading of aminosilanes. Indeed, the conventional synthesis of SBA-15 uses a templating tri-block co-polymer [16,17] that has ends that extend out of the micellar structures to form micropores. The micropore volume of SBA-15 can be reduced using different methods, including increasing the hydrothermal treatment temperature. [24] The removal of the micropores was shown by Kane et al. to improve the catalytic activity for tertiary amine catalysts for the Knoevenagel reaction. [47] Whereas SBA-15 has micropores, MCM-41 is an attractive material because its synthesis results in materials without micropores; however, MCM-41 has smaller pores sizes than SBA-15. The small pores of MCM can impact cooperative amine-silanol interactions. [48] Tailoring the acid and base interactions by tuning the structure of the support will help to develop cooperative catalysts with favorable amine-silanol interactions.

Along with the aminosilane and support structures, the surface loading of amines can impact the catalytic activity. [22,29] As the loading of the aminosilane increases, there are fewer silanols available to participate in the amine-silanol cooperative interaction. [22] Whereas previous work had speculated that amine clustering at high surface densities reduced catalytic activity, [22] Chen et al. used site quantification experiments to demonstrate that aminosilica materials had four types of sites that each exhibited distinct catalytic activity. [49] The materials were found to have four types of sites: (1) high activity, (2) medium activity, (3) low activity, and (4) inactive. The fraction of these different sites was affected by the surface loading. As the surface loading increased beyond 0.7 mmol/g, the activity started to decrease because of amine clustering and silanol consumption that limited beneficial cooperative interactions. The quantification of the activity of these sites is important to understanding the activity of cooperative partners. This understanding provides synthetic targets to enable creating more active catalytic materials.

The impact of cooperative interactions in aminosilica materials have been primarily investigated using MCM-41 and SBA-15. MCM-41 and SBA-15 are considered model 2-dimensional materials. However, recent work has suggested that molecular interactions between the substrates and the silanol surface may influence molecular diffusion in the pores. [50] Although SBA-15 and MCM-41 have been tested for diffusion limitations [35,48] that have been further evaluated using Weisz-Prater criteria, the observed reaction rates could be impacted by molecular diffusion. The diffusion limitations can be mitigated by using a 3-dimensional structure, such as MCM-48, where the added dimensionality would increase the accessibility of sites. MCM-48 is a 3-dimensional version of MCM materials that has interwoven tubular pores similar to the pores of MCM-41. [51] Understanding the impact of these different support structures will help the development of highly active heterogenous catalysts for aldol chemistry.

In this work, we investigate the impact of the structure of mesoporous materials on the catalytic activity using three common mesoporous silica materials. The materials are synthesized, functionalized, and characterized using standard methods, including nitrogen physisorption, XRD, and elemental analysis. The characterized materials are tested for catalytic activity for the aldol reaction and condensation between 4-nitrobenzaldehyde and acetone. The materials are tested using site quantification experiments that involve adding controlled amounts of methane sulfonic acid to selectively deactivate a fraction of the sites. The experiments are used to quantify the activity of each material on a per site basis to gain insights into the behavior of these types of catalysts. Overall, the results reveal the per site activity for different common mesoporous silica catalyst supports.

2. Experimental methods

2.1. Chemicals

All chemicals are used as received. The chemicals used are: tetraethyl orthosilicate (TEOS; 98%, Acros Chemical), cetyltrimethylammonium bromide (CTAB; Amresco), butanol (99%, Alfa Aesar), ammonium hydroxide (28–30%, Sigma Aldrich), sodium hydroxide (GFS), hydrochloric acid (36.5–38%, VWR), poloxamer P-123 (Sigma Aldrich), methane sulfonic acid (98%, Alfa Aesar), ethyl acetate (ACS Grade, Fisher), N-methyl-3-aminopropyl trimethoxy silane (MAPS; Gelest), acetone (HPLC Grade, J.T. Baker), 4-nitrobenzaldehyde (99%, Acros Chemical), 1,3,5-trimethoxybenzene (98%, TCI), and house supplied DI water.

2.2. Material synthesis and characterization

The bare silica supports are synthesized using standard methods for MCM-41, [52,53] SBA-15, [54,55] and MCM-48. [56,57] For the SBA-15, the micropore content can be limited by modifying the static hydrothermal treatment conditions. SBA-15 made using typical conditions is labeled REG-SBA-15 whereas the negligible-micropore SBA-15 is labeled NMP-SBA-15. The detailed synthesis procedures can be found in the supplementary information. Additionally, the bare materials are functionalized with an organosilane using methods described previously. [35,58,59] The grafted materials are labelled using the type of amine and the type of support. For a secondary amine grafted onto MCM-41, the material is labelled 2°Am-MCM-41.

These materials are characterized using N_2 physisorption, x-ray diffraction spectroscopy (XRD), and elemental analysis. The detailed

characterization procedures can be found in the supplementary information. The methods are used to characterize both the bare and grafted materials.

2.3. Catalytic testing and site quantification experiments - Aldol reaction and condensation

The materials are tested for catalytic activity in the aldol condensation of 4-nitrobenzaldehyde and acetone, with 1,3,5-trimethoxybenzene as internal standard. A bulk solution with the reactants is prepared with 4-nitrobenzaldehyde (75.6 mg) and 1,3,5-trimethoxybenzene (40 mg) in 10 mL of acetone. The catalytic testing is performed as described in previous work [49] and is described in more detail in the supplementary information.

The materials are also investigated using a series of site quantification experiments. In addition to the bulk solution for catalytic testing, a solution of methane sulfonic acid (MSA) in ethyl acetate is prepared with a concentration of MSA to poison 100% of the active sites in 500 μL. The poisoning solution is prepared using serial dilution with ethyl acetate, which has previously been identified as a solvent for site quantification experiments. [49] First, a solution (solution A) is prepared with 39.7 μL of MSA in 1960.3 μL ethyl acetate using a combination of 100 μL and 1000 μL micropipettes. Then, 200 μL of solution A is added to 5800 μL of ethyl acetate for the final solution.

For each test, the reactor consists of a 10 mL 2-neck round bottom flask fitted with a condenser with both openings being sealed with a septum. The catalyst is added to the flask with the mass of catalyst adjusted to achieve 5 mol%. The MSA solution and pure ethyl acetate are added to the flask with the catalyst based on the desired poisoning level with a combined total volume of 200 μL. Once the ethyl acetate and MSA solution are added, mixtures are stirred for ~60 s before the 2 mL of the kinetic testing solution is added. MSA is a suitable poison for site quantification experiments as it has limited to no binding to bare NMP-SBA-15 and interacts with 2°Am-NMP-SBA-15, as shown using DRIFTS in Figure S6. Once the reaction mixture is added, the mixture is stirred for another 30 s, then a 50 μL sample is taken, and filtered using a silica plug filter and is used as the initial point (t_0). The flask is then immersed in a silicone oil bath that has been pre-heated to 40 °C with a Heidolph hot plate stirrer. The following procedure is the same as a normal kinetic testing procedure as mentioned in the supplementary information.

3. Results and discussion

3.1. Material characterization

The mesoporous silica materials are successfully synthesized, as demonstrated using nitrogen physisorption and XRD. The calcined materials are characterized with XRD, as shown in Figure S3. The results are described in more detail in the supplementary information and are consistent with previous work synthesizing these materials. Nitrogen physisorption is used to characterize the textural properties of the materials, as reported in Figure S4a and S5a. All materials exhibit type IV adsorption isotherms with REG-SBA-15 [54,55] and NMP-SBA-15 [35, 60] showing hysteresis. These isotherms are consistent with reported literature. [52,53,61].

The adsorption isotherms are used to calculate the BET surface area, micropore content, and pore sizes, as summarized in Table 1. The MCM materials have the largest surface area; MCM-41 and MCM-48 both have a BET surface area of 1110 m^2/g. The NMP-SBA-15 material is found to have a BET surface area of 540 m^2/g. Figure S4a shows the physisorption isotherm for REG-SBA-15, which has a BET surface area of 930 m^2/g.

The adsorption isotherm is analyzed using the BdB-FHH method [62] to determine the pore size distributions of all materials, as shown in Figure S4b and S5b. MCM-41 and MCM-48 have the smallest pore sizes with pore diameters of 3.3 nm and 2.8 nm, respectively. Moreover, the calculated pore diameters for REG-SBA-15 and NMP-SBA-15 have much larger pore diameters of 7.1 and 8.5 nm, respectively. The MCM and SBA-type materials all are found to have highly uniform pore structures and high surface areas.

Since our recent work demonstrates that the micropore volume can impact the catalytic activity, [35,47] the adsorption isotherms are used to calculate the *t*-plot analysis to determine the micropore volume. The MCM materials are determined to have limited to no micropore volume. This is distinct from REG SBA-15 that has a micropore volume of 0.08 cm^3/g. The synthesis modification for SBA-15 is effective in producing a material with limited to negligible micropore volume as NMP-SBA-15 has a micropore volume of 0.001 cm^3/g. The characterization data demonstrate the successful synthesis of the target mesoporous materials.

The bare materials are functionalized using the grafting method and are characterized using N_2 physisorption, XRD, and elemental analysis. Elemental analysis supports the successful grafting of the aminosilane on the silica surface. The target is to synthesize materials with similar surface densities of amines since it is known that amine-silanol interactions are beneficial for this reaction. The surface density of all materials is around 0.43 μmol m^2, as listed in Table 1. Aminosilane grafting reduces the total nitrogen uptake of each of the materials, as shown in Fig. 1a. Table 1 summarizes the BET surface area, micropore content, pore size, and nitrogen loading for the grafted materials. In all materials, their respective surface area and pore size are reduced. As shown in Fig. 1b, each material has a reduced pore diameter compared to the respective bare material since the aminosilane occupies space inside the mesopores. The *t*-plot analysis for these materials shows that all remaining micropores are filled or blocked by the attached

Table 1
Summary of N_2 physisorption and elemental analysis for grafted MCM-48, MCM-41, NMP SBA-15, and REG SBA-15.

Material	BET SA (m^2/g)[a]	Micropore area (m^2/g)[b]	Micropore volume (cm^3/g)[b]	Pore diameter (nm)[c]	Amine loading (mmol/g)[d]	Surface density (μmol/m^2)[e]
MCM-48	1110	–	0	2.8	–	–
2°Am-MCM-48	1000	–	0	2.5	0.471	0.424
MCM-41	1110	–	0	3.1	–	–
2°Am-MCM-41	970	–	0	3.0	0.507	0.456
NMP-SBA-15	540	6.1	0.001	8.5	–	–
2°Am-NMP-SBA-15	425	–	0	8.1	0.257	0.476
REG SBA-15	930	190	0.08	7.1	–	–
2°Am-REG-SBA-15	740	79	0.03	6.8	0.378	0.402

[a] Calculated from N_2 physisorption adsorption isotherm;
[b] Calculated from N_2 physisorption t-plot analysis;
[c] Calculated from N_2 physisorption adsorption isotherm using the BdB-FHH method;
[d] Elemental analysis nitrogen loading;
[e] Nitrogen loading normalized to the material surface area

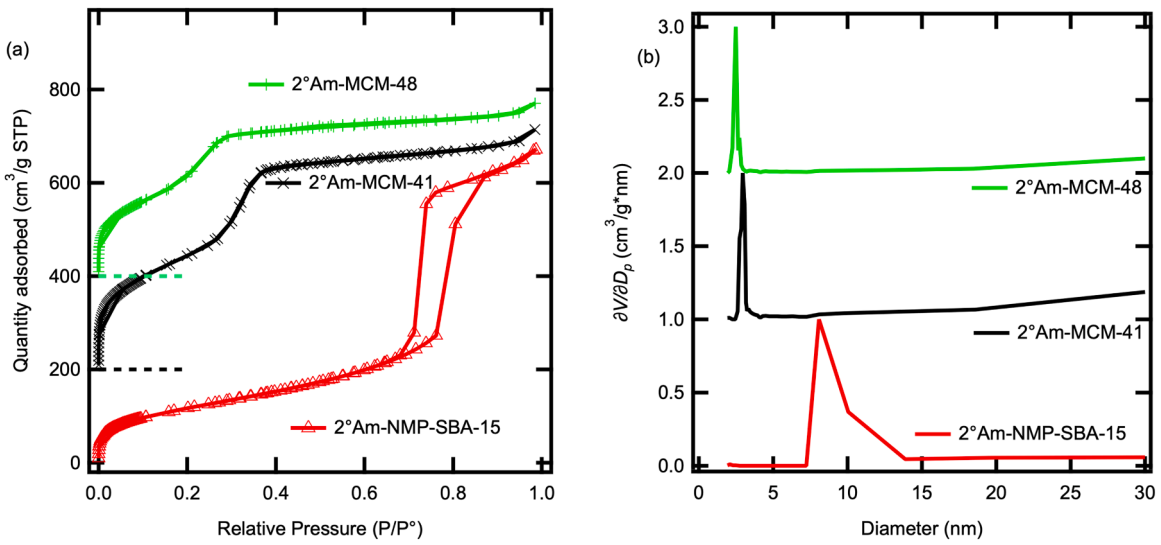

Fig. 1. (a) Comparison of the N_2 Physisorption for grafted MCM-48, MCM-41, and NMP SBA-15. The data is offset for MCM-48 (400) and MCM-41 (200) for clarity of each isotherm. (b) Comparison of the respective pore size distributions normalized to a maximum value of one.

organosilane for the SBA materials. Overall, the reduction in the surface areas and pore diameters are consistent with expectations for post-grafted materials.

3.2. Catalytic activity

The grafted materials are tested for catalytic activity in the aldol reaction and condensation between 4-nitrobenzaldehyde and acetone. The material 2°Am-REG-SBA-15 is used as a basis for comparison. The data is shown for the fractional conversion as a function of time from the 0:1 MSA:2°Am results, as shown in Fig. 2. The conversion data can be fit with a first order model to determine an observed rate constant. For 2°Am-REG-SBA-15, the first order rate constant is calculated to be 0.2 hr^{-1}, as listed in Table 2. This is consistent with our recent results investigating secondary amines on mesoporous SBA-15. [48] These

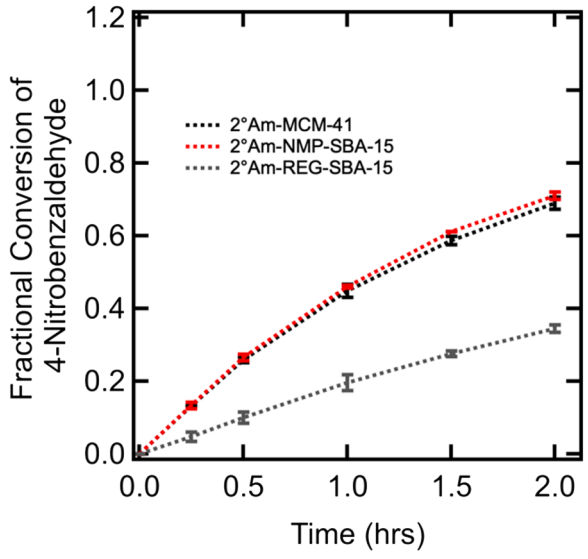

Fig. 2. Comparison of the fractional conversion of 4-nitrobenzaldehyde over time for grafted MCM-41, NMP-SBA-15, and REG-SBA-15 for the aldol reaction and condensation with acetone. Each material is tested with a reaction solution containing 0.05 mmol/mL of 4-nitrobenzaldehyde and 0.024 mmol/mL of 1,3,5-trimethoxybenzene (internal standard) in 2 mL acetone, and a 5 mol% catalyst loading (based on elemental analysis) relative to 4-nitrobenzaldehyde.

Table 2
Summary of the observed rate constants for MCM-48, MCM-41, REG-SBA-15, and NMP-SBA-15. The errors are calculated as the standard deviation of multiple catalytic tests.

Material	k_{obs} (hr^{-1})
2°Am-REG-SBA-15	0.20 ± 0.002
2°Am-NMP-SBA-15	0.62 ± 0.002
2°Am-MCM-41	0.60 ± 0.03
2°Am-MCM-48	0.49 ± 0.02

results are compared to the kinetic testing results for 2°Am-MCM-41 and 2°Am-NMP-SBA-15 that are found to have observed reaction rate constants of 0.6 and 0.62 hr^{-1}, respectively. Interestingly, the 2°Am-NMP material has three times the catalytic activity of 2°Am-REG material, which is consistent with our previous results for aldol chemistry for biomass derived compounds. [35] Previously, we have attributed this difference to aminosilane grafting in the micropores of material, resulting in inactive catalytic sites. Interestingly, the observed reaction rate constants are similar for the aldol reaction and condensation for 2°Am-MCM-41 and 2°Am-NMP SBA-15. Both materials have limited to no micropore volume, consistent with the hypothesis that materials with limited micropore volume have higher average catalytic activity than materials with micropores.

The catalytic activity for the two-dimensional material is compared to the catalytic activity of MCM-48. Although the kinetic testing for the two-dimensional materials demonstrate that the results are not mass transfer limited, it may be possible that molecular interactions of the substrates with the silica surface could impact diffusion in the material, which would be reduced with access in all three dimensions. As shown in Figs. 3, 2°Am-MCM-48 has is less active than 2°Am-MCM-41 (2°Am-MCM-41 k_{obs} = 0.60 ± 0.03 hr^{-1} and 2°Am-MCM-48 k_{obs} = 0.49 ± 0.02 hr^{-1}). These rates are comparable to literature [28,31,63] given the differences in reaction conditions and testing methods. From the GC-FID result, the aldol reaction product is more selectively formed than the condensation product for all the three materials (as shown in Table S1) with an approximate selectivity of 80% for the reaction product. Overall, the results demonstrate that 2°Am-MCM-41, 2°Am-MCM-48, and 2°Am-NMP-SBA-15 are highly active. Additional site quantification experiments will provide key insights about the differences in activity observed for the materials.

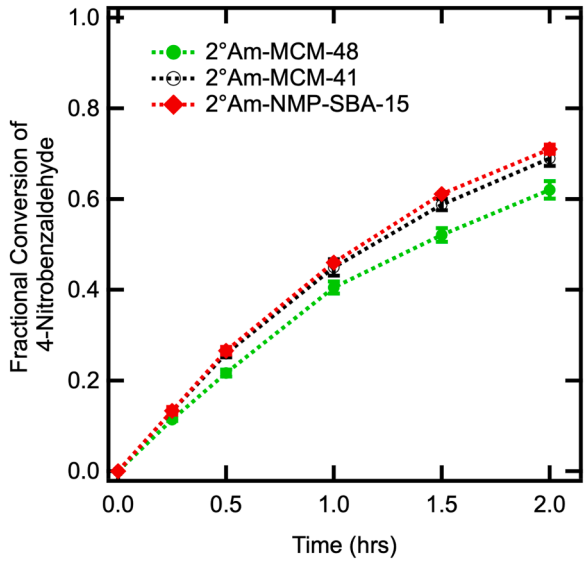

Fig. 3. Comparison of the fractional conversion of 4-nitrobenzaldehyde over time for grafted MCM-48, MCM-41, and NMP SBA-15 for the aldol reaction and condensation with acetone. Each material is tested with a reaction solution of 0.05 mmol/mL 4-nitrobenzaldehyde and 0.024 mmol/mL 1,3,5-trimethoxybenzene in 2 mL acetone, and a 5 mol% catalyst loading relative to 4-nitrobenzaldehyde.

3.3. Site quantification experiments

The materials are tested using site quantification experiments to determine the fraction and types of active sites in the material. The experiments involve the addition of different ratios of methane sulfonic acid to the 2° amine functionalized material to deactivate a fraction of the sites. The conversion over time plots for the different materials using different amounts of MSA are shown in Figure S7 to S9. As shown in Fig. 4, the observed reaction rate constant for 2°Am-NMP-SBA-15 monotonically decreases with addition of the MSA solution. Ideally, the 2°Am-NMP-SBA-15 material would reach 0% activity at a poisoning ratio of 1; however, the material reaches 0% activity around a poisoning ratio of 0.7, indicating that a fraction of sites is inactive. This observation demonstrates that all sites are not active in these materials. Interestingly, the data have two slopes that includes a sharp initial decrease in activity that begins to level off as the poisoning ratio increases. The site quantification data for a catalyst with the same type of reaction sites would occur linearly; however, the deactivation of 2°Am-NMP-SBA-15 occurs with multiple slopes. The differences in the slopes as the poisoning ratio increases suggests that there are at least two different types of active sites present.

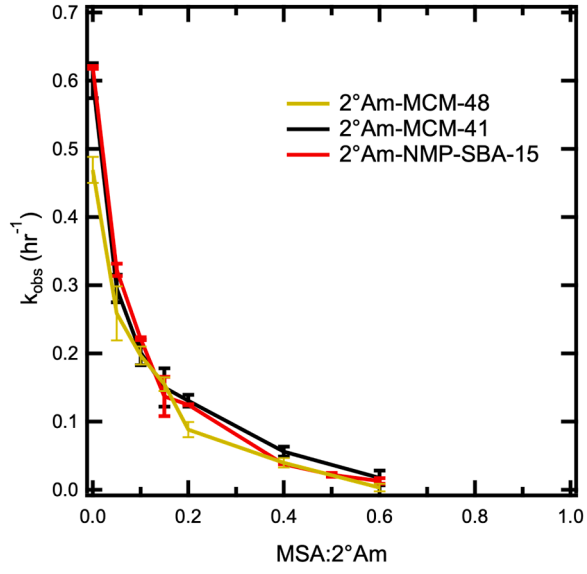

Fig. 4. Comparison of the k_{obs} as a function the poisoning ratio of MSA: 2°Am-MCM-48, 2°Am-MCM-41, and 2°Am-NMP SBA-15 for the aldol reaction and condensation with acetone. Each material is tested with a reaction solution of 0.05 mmol/mL 4-nitrobenzaldehyde and 0.024 mmol/mL 1,3,5-trimethoxybenzene in 2 mL acetone, a poisoning solution having a concentration of 0.01 mmol MSA/mL ethyl acetate added relative to the desired poisoning level, and a 5 mol% catalyst loading relative to 4-nitrobenzaldehyde.

The remaining materials are tested using site quantification experiments, as shown in Fig. 4. Each material had a sharp initial decrease in activity that flattens as the poisoning ratio increases. The 2°Am-MCM-48 material is found to have about 60% of sites active whereas 2°Am-MCM-41 and 2°Am-NMP-SBA-15 have about 70% of sites active. These quantities of active sites are similar to 2°Am-NMP-SBA-15 that is likely because these materials have limited micropore volume. Further, each of these materials have high activity sites, demonstrating that all aminosilica materials have high activity sites.

The site quantification data is further analyzed through fitting the data using a four-site model to determine the activity and fraction of active sites. A four-site model is selected since our previous work demonstrated that four distinct types of sites exists. [49] In the model, there are three types of sites that are active for the reaction – high activity, medium activity, and low activity – and one inactive site. The fit equation for the observed reaction rate constant (k_{obs}) is:

$$k_{obs} = f_1k_1 + f_2k_2 + f_3k_3 + f_4k_4 \quad (1)$$

where k_{obs} is the observed reaction rate constant for a first order reaction, f_n is the fraction of sites of type n, and k_n is the first order rate constant for site n. The model assumes that each type of site will exist in each material and will have the same rate constant in each material. [49] More detail for model fitting is described in the supplementary information.

The fitted observed rate constants of these sites are shown in Table 3 and Fig. 5. The four-site model fits the data well. The highly active sites are associated with the first slope in Fig. 4 and are titrated by the methane sulfonic acid at low concentrations of the acid. The medium and low activity sites can be observed at moderate and high poisoning levels. The rate constant for the high activity site (k_1 = 6.12 hr^{-1}) is significantly higher than the rate constant for the medium (k_2 = 0.83 hr^{-1}) and low activity (k_3 = 0.16 hr^{-1}) sites. All four materials exhibited each type of site, but the fraction of each type of site is different.

Quantifying the distribution of active sites for a catalytic material provides insights on the behavior of the catalysts. As shown in Fig. 5(a), the data are presented for the fraction of each type of site for each material. 2°Am-MCM-41 has the highest fraction of active sites (73%). 2°Am-NMP-SBA-15 and 2°Am-MCM-48 material have similar quantities of total active sites of 65% and 63%, respectively. Whereas the synthesis of NMP-SBA-15 and the MCM materials produces materials with limited

Table 3
Summary of the calculated rates of reaction and fraction of each type of site for the range of mesoporous materials tested using site quantification experiments.

Material	f_1 (k_1 = 6.12 ± 0.24)	f_2 (k_2 = 0.83 ± 0.08)	f_3 (k_3 = 0.16 ± 0.05)	f_1+f_2+f_3
2°Am-NMP-SBA-15	0.063 ± 0.003	0.22 ± 0.03	0.37 ± 0.07	0.65
2°Am-MCM-41	0.06 ± 0.003	0.19 ± 0.03	0.49 ± 0.09	0.73
2°Am-MCM-48	0.043 ± 0.003	0.21 ± 0.03	0.38 ± 0.07	0.63

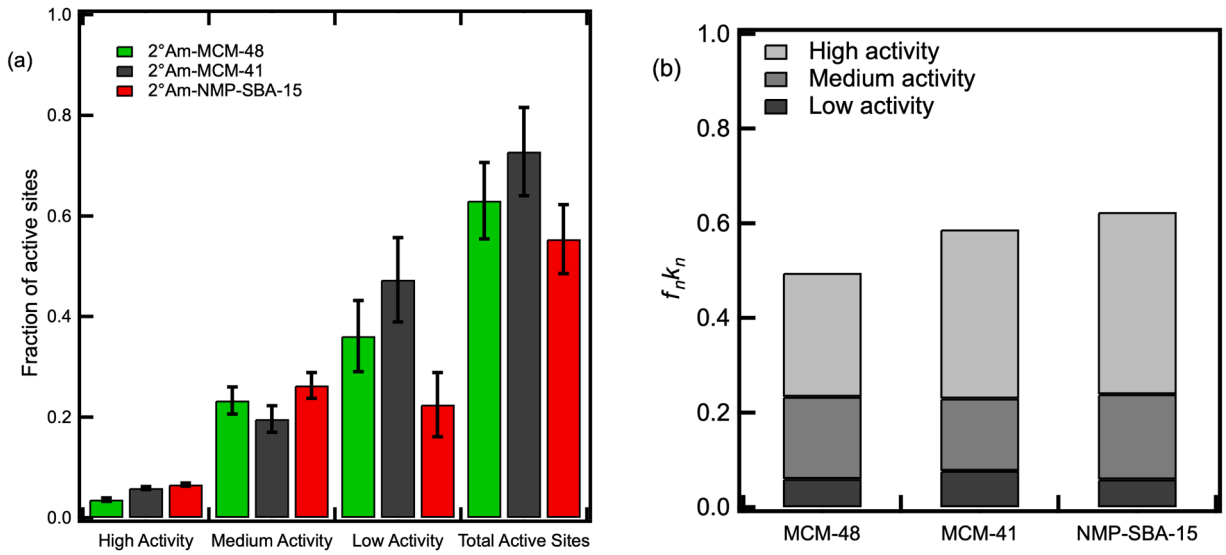

Fig. 5. (a) Comparison of the fraction of sites for 2°Am-MCM-48, 2°Am-MCM-41, and 2°Am-NMP SBA-15 organized by the type of active site. (b) Comparison of the activity contribution for each type of active site towards the observed catalytic activity for 2°Am-MCM-48, 2°Am-MCM-41, and 2°Am-NMP-SBA-15.

micropore volume, a fraction of the amines is still inactive, suggesting potential targets for improvement.

Increasing the fraction of high activity sites is desirable for developing highly efficient catalysts. Indeed, the contribution of each type of site (n) to k_{obs} can be calculated as $f_n k_n$. The contribution of each type of site is depicted in Fig. 5b. Even though the high activity sites represent a small fraction, the high active sites have the largest contribution to the observed catalytic activity for all materials. Both, 2°Am-MCM-41 and 2°Am-NMP SBA-15 have a similar number of highly active sites. Interestingly, 2°Am-MCM-48 has fewer high activity sites compared to 2°Am-MCM-41, causing 2°Am-MCM-48 to be measurably less active than 2°Am-MCM-41. The large contribution of high activity sites highlights the importance of minority species to the overall richness and high activity of these catalytic materials.

The remainder of the catalytic activity is associated with the medium and low activity sites. Combined, the medium and low activity sites contribute to approximately 50% or less of the observed catalytic activity for all materials tested, as shown in Fig. 5b. Our previous work has shown that the low activity sites are associated with amine clusters that lack amine-silanol cooperative interactions. [49] The 2°Am-NMP-SBA-15 is found to have more low activity sites (37%) than medium activity sites (22%). These results are consistent with previous reports for these materials under these reaction conditions. [1,9] 2°Am-MCM-41 is found to have the largest fractions of low and medium activity sites. Although 2°Am-MCM-41 has a large fraction of active sites, the sites have medium or low activity that provide a smaller benefit to the overall activity than the highly active sites. Currently, it is unclear what the difference is between the medium and high activity sites. In our previous work, we eliminated two possible hypotheses for the structure of high activity sites: (1) amines grafted in pairs, and (2) amines grafted on the external surface. Ongoing work is investigating the difference between the high and medium activity sites. We have speculated that the difference may be associated with the type of silanol (i.e., isolated or vicinal) involved in the cooperative interaction, but this hypothesis is currently being tested.

The rate constant for the medium and low activity sites are similar to results for our previous work. [49] Yet, the rate constant for the high activity site ($k_1 = 6.12\ hr^{-1}$) is higher than our previous work ($k_1 = 1.7\ hr^{-1}$). In examining the differences in catalytic testing methods and results, a key difference is the reaction temperature where our previous work uses 40 °C and here is 50 °C. Likely, the discrepancies represent subtle differences in experimental methodology between researchers for these time consuming and challenging experiments. Yet, the current work supports that the materials have multiple types of sites with high activity sites contributing significantly to the overall observed catalytic activity.

4. Conclusions

Three different types of amine-functionalized mesoporous silica materials are used to demonstrate that different supports will exhibit different types of reaction sites in different quantities. The materials are synthesized using common methods and an adapted method to limit the micropore content of SBA-15. The 2°Am-MCM-41 material is found to have the highest fraction of overall active sites whereas the 2°Am-NMP-SBA-15 material is found to have the highest amount of highly active sites. With the added dimension for the MCM-48 material, there was a reduction of the low activity sites and an increase in the amount of medium activity sites, but at the cost of the more desirable highly active sites. Reducing the micropores in NMP SBA-15 produces a catalytic material with similar activity to MCM-41. Synthesizing catalysts with higher fractions of the high and medium activity sites is imperative to developing more effective and complex catalysts.

CRediT authorship contribution statement

Mike Brizes: Methodology, Validation, Formal analysis, Investigation, Data curation, Writing – original draft, Writing – review & editing, Visualization. **Jee-Yee Chen:** Conceptualization, Formal analysis, Investigation, Writing – original draft, Writing – review & editing. **Hannah Pineault:** Methodology, Investigation, Writing – original draft, Writing – review & editing. **Nicholas Brunelli:** Conceptualization, Validation, Formal analysis, Writing – original draft, Writing – review & editing, Visualization, Supervision, Project administration, Funding acquisition.

Declaration of Competing Interest

The authors declare that they have no known competing financial interests or personal relationships that could have appeared to influence the work reported in this paper.

Data Availability

Data will be made available on request.

Acknowledgements

We acknowledge the National Science Foundation (grants 2015669 and 1933054) for the financial support.

Appendix A. Supporting information

Supplementary data associated with this article can be found in the online version at doi:10.1016/j.apcata.2022.118997.

References

[1] A. Policicchio, G. Conte, R.G. Agostino, P. Caputo, C. Oliviero Rossi, N. Godbert, I. Nicotera, C. Simari, J. CO_2 Util. 55 (2022), 101809.
[2] V. Zeleňák, M. Badaničová, D. Halamová, J. Čejka, A. Zukal, N. Murafa, G. Goerigk, Chem. Eng. J. 144 (2008) 336–342.
[3] A. Popa, S. Borcanescu, I. Holclajtner-Antunović, D. Bajuk-Bogdanović, S. Uskoković-Marković, J. Porous Mater. 28 (2021) 143–156.
[4] E.S. Sanz-Pérez, C.R. Murdock, S.A. Didas, C.W. Jones, Chem. Rev. 116 (2016) 11840–11876.
[5] J.C. Hicks, J.H. Drese, D.J. Fauth, M.L. Gray, G. Qi, C.W. Jones, J. Am. Chem. Soc. 130 (2008) 2902.
[6] S. Wang, Microporous Mesoporous Mater. 117 (2009) 1–9.
[7] R.F. Popovici, E.M. Seftel, G.D. Mihai, E. Popovici, V.A. Voicu, J. Pharm. Sci. 100 (2011) 704–714.
[8] D. Brunel, Microporous Mesoporous Mater. 27 (1999) 329–344.
[9] R.K. Zeidan, S.-J. Hwang, M.E. Davis, Angew. Chem. Int. Ed. 45 (2006) 6332–6335.
[10] A.J. Crisci, M.H. Tucker, J.A. Dumesic, S.L. Scott, Top. Catal. 53 (2010) 1185–1192.
[11] I.K. Mbaraka, B.H. Shanks, J. Catal. 229 (2005) 365–373.
[12] D.M. Ford, E.E. Simanek, D.F. Shantz, Nanotechnology 16 (2005) S458–S475.
[13] F. Zhang, Y. Yan, H. Yang, Y. Meng, C. Yu, B. Tu, D. Zhao, J. Phys. Chem. B 109 (2005) 8723–8732.
[14] R. Ryoo, S. Jun, J. Phys. Chem. B 101 (1997) 317–320.
[15] J.M. Kim, J.H. Kwak, S. Jun, R. Ryoo, J. Phys. Chem. 99 (1995) 16742–16747.
[16] D. Zhao, Q. Huo, J. Feng, B.F. Chmelka, G.D. Stucky, J. Am. Chem. Soc. 120 (1998) 6024–6036.
[17] D. Zhao, J. Feng, Q. Huo, N. Melosh, G.H. Fredrickson, B.F. Chmelka, G.D. Stucky, Sci. (80-.). 279 (1998) 548–552.
[18] J.S. Beck, J.C. Vartuli, W.J. Roth, M.E. Leonowicz, C.T. Kresge, K.D. Schmitt, C.T.-W. Chu, D.H. Olson, E.W. Sheppard, S.B. McCullen, J.B. Higgins, J.L. Schlenker, J. Am. Chem. Soc. 114 (1992) 10834–10843.
[19] C.T. Kresge, M.E. Leonowicz, W.J. Roth, J.C. Vartuli, J.S. Beck, Nature 359 (1992) 710–712.
[20] J.D. Bass, A. Solovyov, A.J. Pascall, A. Katz, J. Am. Chem. Soc. 128 (2006) 3737–3747.
[21] N.A. Brunelli, S.A. Didas, K. Venkatasubbaiah, C.W. Jones, J. Am. Chem. Soc. 134 (2012) 13950–13953.
[22] J. Lauwaert, E. De Canck, D. Esquivel, J.W. Thybaut, P. Van Der Voort, G.B. Marin, ChemCatChem 6 (2014) 255–264.
[23] Q. Wang, V.V. Guerrero, A. Ghosh, S. Yeu, J.D. Lunn, D.F. Shantz, J. Catal. 269 (2010) 15–25.
[24] A. Galarneau, H. Cambon, F. Renzo, R. Ryoo, M. Choi, F. Fajula, N. J. Chem. 27 (2003) 73–79.
[25] R.K. Zeidan, M.E. Davis, J. Catal. 247 (2007) 379–382.
[26] K. Kandel, S.M. Althaus, C. Peeraphatdit, T. Kobayashi, B.G. Trewyn, M. Pruski, I. I. Slowing, ACS Catal. 3 (2013) 265–271.
[27] D. Singappuli-Arachchige, T. Kobayashi, Z. Wang, S.J. Burkhow, E.A. Smith, M. Pruski, I.I. Slowing, ACS Catal. 9 (2019) 5574–5582.
[28] J. Lauwaert, E.G. Moschetta, P. Van Der Voort, J.W. Thybaut, C.W. Jones, G. B. Marin, J. Catal. 325 (2015) 19–25.
[29] N.A. Brunelli, C.W. Jones, J. Catal. 308 (2013) 60–72.
[30] N.A. Brunelli, K. Venkatasubbaiah, C.W. Jones, Chem. Mater. 24 (2012) 2433–2442.
[31] J. Lauwaert, E. De Canck, D. Esquivel, P. Van Der Voort, J.W. Thybaut, G.B. Marin, Catal. Today 246 (2015) 35–45.
[32] A. De Vylder, J. Lauwaert, J. De Clercq, P. Van Der Voort, J.W. Thybaut, J. Catal. 361 (2018) 51–61.
[33] S. Bahmanyar, K.N. Houk, V. Uni, L. Angeles, R.V. July, J. Am. Chem. Soc. (2001) 12911–12912.
[34] J.N. Chheda, G.W. Huber, J.A. Dumesic, Angew. Chem. Int. Ed. 46 (2007) 7164–7183.
[35] J.-Y. Chen, N.A. Brunelli, Energy Fuels 35 (2021) 14885–14893.
[36] S. Van de Vyver, C. Odermatt, K. Romero, T. Prasomsri, R. Rodríguez, ACS Catal. 5 (2015) 972–977.
[37] K. Ponnuru, J.C. Manayil, H.J. Cho, W. Fan, K. Wilson, F.C. Jentoft, ChemPhysChem 19 (2018) 386–401.
[38] W.-D. Fessner, A. Schneider, H. Held, G. Sinerius, C. Walter, M. Hixon, J.V. Schloss, Angew. Chem. Int. Ed. 35 (1996) 2219–2221.
[39] R.D. Kobes, R.T. Simpson, B.L. Vallee, W.J. Rutter, Biochemistry 8 (1969) 585–588.
[40] H.J.M. Gijsen, L. Qiao, W. Fitz, C.-H. Wong, Chem. Rev. 96 (1996) 443–473.
[41] E.G. Moschetta, N.A. Brunelli, C.W. Jones, Appl. Catal. A, Gen. 504 (2015) 429–439.
[42] Y. Kubota, K. Goto, S. Miyata, Y. Goto, Y. Fukushima, Y. Sugi, Chem. Lett. 32 (2003) 234–235.
[43] J.D. Bass, S.L. Anderson, A. Katz, Angew. Chem. Int. Ed. 115 (2003) 5377–5380.
[44] S. Shylesh, D. Hanna, J. Gomes, C.G. Canlas, M. Head-Gordon, A.T. Bell, ChemSusChem 8 (2015) 466–472.
[45] K.C. Kim, E.G. Moschetta, C.W. Jones, S.S. Jang, J. Am. Chem. Soc. 138 (2016) 7664–7672.
[46] A. De Vylder, J. Lauwaert, M.K. Sabbe, M.F. Reyniers, J. De Clercq, P. Van Der Voort, J.W. Thybaut, Chem. Eng. J. 404 (2021), 127070.
[47] A. Kane, N. Deshpande, N.A. Brunelli, AIChE J. 65 (2019), e16791.
[48] N. Deshpande, J.-Y. Chen, T. Kobayashi, E.H. Cho, L.-C. Lin and N.A. Brunelli, *(in Rev.*
[49] J.-Y. Chen, H. Pineault, N.A. Brunelli, J. Catal. 413 (2022) 1048–1055.
[50] Y.L. Kim, J.W. Evans and M. Gordon, *Phys. Chem. Chem. Phys.*, DOI:10.1039/d2cp00952h.
[51] A. Monnier, F. Schüth, Q. Huo, D. Kumar, D. Margolese, R.S. Maxwell, G.D. Stucky, M. Krishnamurty, P. Petroff, A. Firouzi, M. Janicke, B.F. Chmelka, Sci. (80-.). 261 (1993) 1299–1303.
[52] M. Laghaei, M. Sadeghi, B. Ghalei, M. Dinari, Prog. Org. Coat. 90 (2016) 163–170.
[53] D. Kumar, K. Schumacher, C. Du Fresne von Hohenesche, M. Grün, K.K. Unger, Colloids Surf. A Physicochem. Eng. Asp. 187–188 (2001) 109–116.
[54] V. Chaudhary, S. Sharma, J. Porous Mater. 24 (2017) 741–749.
[55] R. Ojeda-López, I.J. Pérez-Hermosillo, J. Marcos Esparza-Schulz, A. Cervantes-Uribe, A. Domínguez-Ortiz, Adsorption 21 (2015) 659–669.
[56] L.A. Solovyov, O.V. Belousov, R.E. Dinnebier, A.N. Shmakov, S.D. Kirik, J. Phys. Chem. B 109 (2005) 3233–3237.
[57] J. Xu, Z. Luan, H. He, W. Zhou, L. Kevan, Chem. Mater. 10 (1998) 3690–3698.
[58] N. Deshpande, L. Pattanaik, M.R. Whitaker, C.-T. Yang, L.-C. Lin, N.A. Brunelli, J. Catal. 353 (2017) 205–210.
[59] N. Deshpande, E.H. Cho, A.P. Spanos, L.-C. Lin, N.A. Brunelli, J. Catal. 372 (2019) 119–127.
[60] W.J.J. Stevens, K. Lebeau, M. Mertens, G. Van Tendeloo, P. Cool, E.F. Vansant, J. Phys. Chem. B 110 (2006) 9183–9187.
[61] M. Thommes, K. Kaneko, A.V. Neimark, J.P. Olivier, F. Rodriguez-Reinoso, J. Rouquerol, K.S.W. Sing, Pure Appl. Chem. 87 (2015) 1051–1069.
[62] P. Schmidt-Winkel, W.W. Lukens, D. Zhao, P. Yang, B.F. Chmelka, G.D. Stucky, J. Am. Chem. Soc. 121 (1999) 254–255.
[63] Y. Kubota, H. Yamaguchi, T. Yamada, S. Inagaki, Y. Sugi, T. Tatsumi, Top. Catal. 53 (2010) 492–499.